3D-printed immunosensor for the diagnosis of Parkinson's disease

Cristiane Kalinke [a,c,*], Paulo Roberto De Oliveira [b,c], Craig E. Banks [c], Bruno Campos Janegitz [b], Juliano Alves Bonacin [a,*]

[a] Institute of Chemistry, University of Campinas (UNICAMP), 13083-859, Campinas, São Paulo, Brazil
[b] Department of Nature Science, Mathematics and Education, Federal University of São Carlos (UFSCar), 13600-970, Araras, São Paulo, Brazil
[c] Faculty of Science and Engineering, Manchester Metropolitan University, Manchester M1 5GD, United Kingdom

Abstract

3D printing technology is a strategic tool for the development of electrochemical sensors and biosensors since it is possible to obtain versatile devices quickly and at a low cost. In this work, an arrangement of 3D-printed electrodes (working, pseudo-reference, and auxiliary) was applied for the detection of PARK7/DJ-1 protein in blood serum and cerebrospinal fluid samples. The immunosensor surface was previously chemically and electrochemically activated to promote the increase of the active sites and the conductivity, allowing the covalent immobilization of the biological species (antibodies) and improving its electrochemical performance. The detection was carried out by impedimetric (5.0 200 μg L^{-1}), and voltammetric measurements (5.0 500 μg L^{-1}), showing limits of detection of 1.01 and 3.46 μg L^{-1}. The 3D-printed immunosensor also achieved good repeatability and reproducibility from normal to abnormal levels of PARK7/DJ-1 protein, aiming for the diagnosis of Parkinson's disease in different stages of the disease.

1. Introduction

3D printing technology has been a useful tool in several research applications and, allied to electrochemical techniques, new sensors and electrochemical devices can be constructed for sensing and biosensing of specific targets [1]. The versatile and rapid prototyping, possibility of different shapes, and miniaturization capability are the main advantages of this approach concerning electrochemical and electroanalytical applications [2,3]. This allows the preparation of electrodes, electrochemical cells, microfluidic and complete electrochemical devices [4-8]. Regarding additive manufacturing, fused deposition modeling (FDM) has been highlighted by its accessibility and possibility of processing a wide range of materials, such as thermoplastic polymers and composite materials [9,10]. Polylactic acid (PLA) is a biodegradable material and has been one of the most used polymers for 3D printing of electrochemical devices, which can be due to its ease of printability, low thermal and environmental impact when compared to other thermoplastics [9,11,12].

PLA-based conductive filaments can naturally present carboxylic groups for the immobilization of biological molecules [13]. However, this interaction can be easily improved by the surface pretreatments of 3D-printed electrodes, mainly by creating active sites and defects on the conductive material [14,15]. Thus, 3D printing has sparked significant progress in the field of diagnosis since point-of-use biosensors can be easily designed to detect antigens. In recent years, 3D-printed biosensors have been reported in the literature exploring different approaches (i.e., by immobilizing enzymes, antibodies, genetic material, and others) aiming the detection of glucose [16], lactate [17], interleukin-6 [18], dengue virus [19], SARS-CoV-2 [20], cancer [21], among others.

The development of biosensors with rapid and reliable responses is of paramount importance to ensure the accurate diagnosis of diseases. Concerning neurodegenerative diseases, such as Parkinson's, the early diagnosis allows for a previous treatment, increasing the chances of curing. One of the ways to detect and/or monitor the progression of Parkinson's disease is related to the levels of the DJ-1 protein, which at low levels can be correlated to the dysregulation of the PARK7 gene expression [22]. DJ-1 protein has an antioxidative neuroprotective role. However, mutations in the PARK7 gene can change the concentration and/or the functionality of the DJ-1 protein, which can be associated with neurological diseases, type 2 diabetes, infertility, and some types of cancer [23,24]. In addition, high levels of oxidation products can be found in the dopaminergic neurons of people diagnosed with Parkinson's disease [25]. This emphasizes the development of rapid and accurate methods for detecting and monitoring species related to

* Corresponding authors at: Institute of Chemistry, University of Campinas (UNICAMP), 13083-859, Campinas, São Paulo, Brazil.
E-mail addresses: cristiane.kalinke@gmail.com (C. Kalinke), jbonacin@unicamp.br (J.A. Bonacin).

neurodegenerative disorders and diseases. In this work, a 3D-printed immunosensor based on treated graphene conducting filament was developed as a proof-of-concept for the detection of PARK7/DJ-1 protein, aiming for Parkinson's disease diagnosis.

2. Experimental

2.1. Reagents and solutions

Phosphate-buffered saline (0.10 mol L^{-1} PBS, pH 7.4) was prepared using potassium phosphate monobasic (>98.0 wt. %), sodium phosphate dibasic (99.0 wt. %), and sodium chloride (99.0 wt. %) from Synth (Diadema, Brazil), and potassium chloride (99.0 wt. %) from Sigma-Aldrich (St. Louis, USA). Ferrocenemethanol (97.0 wt. %, Sigma-Aldrich) prepared in 0.10 mol L^{-1} potassium chloride (99.0 wt. %, Vetec, Brazil) was used as the electrochemical probe. Sodium hydroxide (98.0 wt. %, Synth) was used for electrode chemical activation treatment. Commercially sterile-filtered human serum (code H4522) from Sigma-Aldrich was used. Synthetic cerebrospinal fluid was freshly prepared by using sodium chloride, potassium chloride, calcium chloride dehydrate (≥99.5 wt. %, Sigma-Aldrich), glucose (≥99.5 wt. %, Sigma-Aldrich), sodium bicarbonate (≥99.0 wt. %, Synth), and urea (99.0 wt.

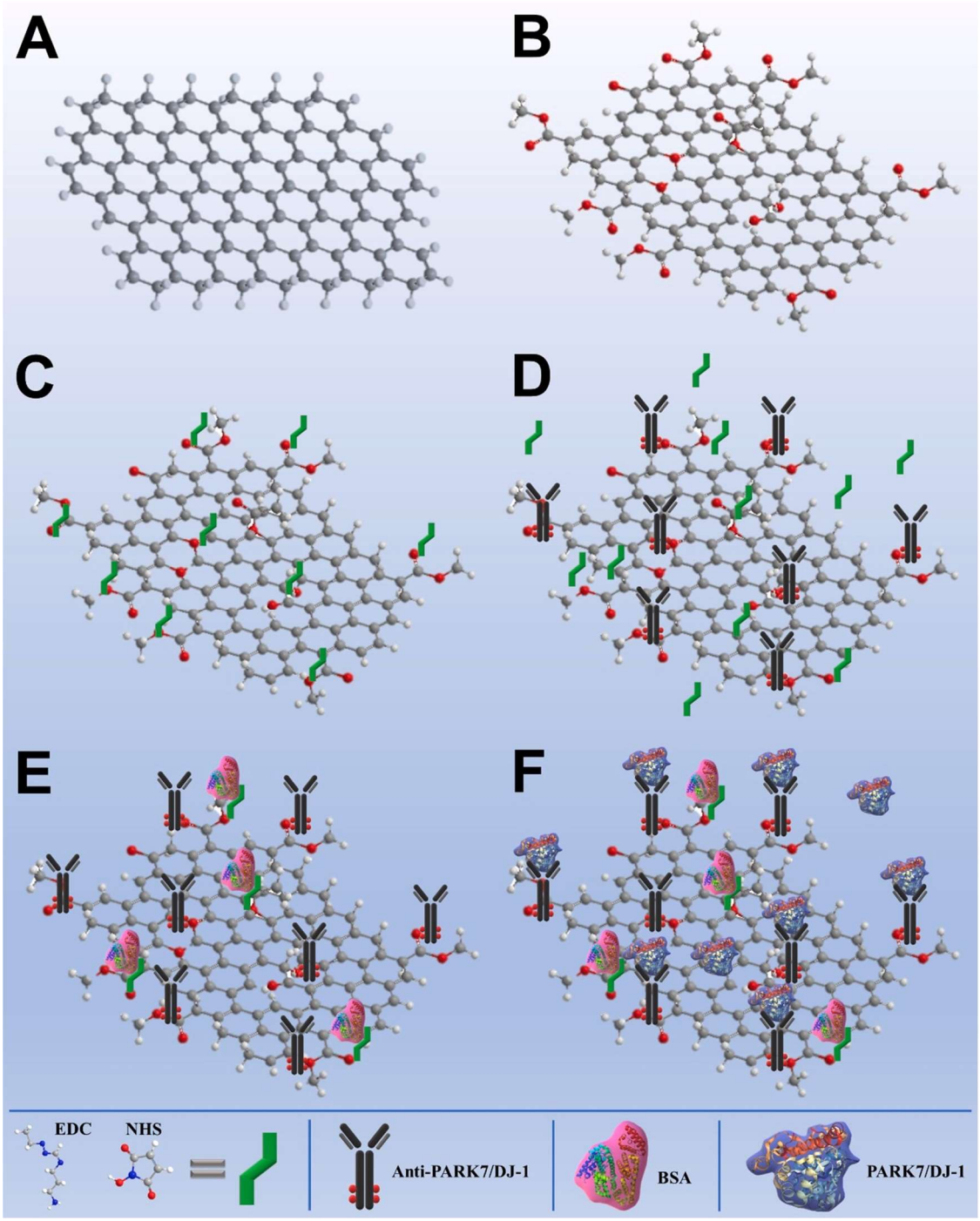

Fig. 1. 3D-printed immunosensor based on graphene immobilization scheme: (A) Before and (B) after chemical + electrochemical activation, (C) EDC/NHS couple incorporation by drop-casting, (D) Anti-PARK7/DJ-1 antibodies immobilization; (E) BSA interaction, and (F) PARK7/DJ-1 antigen interaction.

%, Vetec) in ultrapure water [26]. The solutions were prepared using Milli-Q ultrapure water with resistivity higher than 18 MΩ cm (Merck Millipore, Burlington, USA).

2.2. Instrumental and apparatus

Morphological characterization of the 3D-printed electrodes obtained before and after activation treatment was performed by using a Jeol JSM-J6360 LV scanning electron microscope (SEM). A Nanosurf Easyscan2 Flex AFM was used for atomic force microscopy (AFM) and Kelvin probe force microscopy (KPFM) analysis in the dry atmosphere with an electrical frequency of 15 kHz and amplitude of 5.0 V. A Pt/Ir coated tip with the resonance frequency of 75 kHz and force constant of 2.8 N m^{-1} was used.

Electrochemical measurements were performed in a Metrohm Autolab PGSTAT 204 potentiostat/galvanostat (Utrecht, Netherlands), controlled by Nova 2.1 software. The electrodes were characterized by cyclic voltammetric (CV) and electrochemical impedance spectroscopic (EIS) measurements in presence of 5.0 mmol L^{-1} ferrocene methanol as the electrochemical probe. CV measurements were carried out at a potential range from −0.50 to + 1.0 V, at a scan rate of 25 mV s^{-1}. EIS measurements were recorded from 100 kHz to 0.10 Hz, with an amplitude of 10 mV. The Randles equivalent circuit was used to adjust the experimental data and determine the charge transfer resistance (R_{ct}) related to the redox reaction of the probe, as demonstrated in Fig. S1.

3D-printed electrodes (working, pseudo-reference, and auxiliary electrodes) were manufactured by Fused Deposition Modeling (FDM) using a conductive filament based on polylactic acid (PLA) and graphene (Black Magic 3D, New York, USA). The electrodes showed a disk format with diameter of 6.0 mm (Fig. S2). A Sethi 3D printer (Campinas, Brazil) was used under the following conditions: printing speed of 1000 mm min^{-1}, extrusion temperature of 200 °C, and bed heated temperature of 70 °C [12,27]. 3D-printed pseudo-reference and counter electrodes were used since no significant variation in the potentials has been observed compared to conventional reference electrodes [27]. The as-printed working electrodes (3D PLA-G) were chemically and electroctrochemically activated to increase their electrochemical performance, following previously reported procedures [14,27] (Fig. 1A-B). For this step, each electrode was immersed in 1.0 mol L^{-1} NaOH solution for 30 min. After, the electrochemical treatments were performed by positive (+1.8 V) and negative (—1.8 V) potential application in supporting electrolyte (0.10 mol L^{-1} PB, pH 7.4). All measurements were carried out after oxygen removal by N_2 purging.

2.3. Immunosensor assembly

The steps taken to evaluate the ability of 3D-printed electrodes for the development of an electrochemical immunosensor for the detection of Parkinson's disease are described below. In this case, the PARK7/DJ-1 protein associated with Parkinson's disease was monitored. EDC (1-ethyl-3-(3-dimethylaminopropyl)carbodiimide) and NHS (N- hydroxysuccinimide) couple was used for the immobilization of the biological species, which allows more stable incorporation, covalently, to the electrode surface (Fig. 1C). 5.0 mmol L^{-1} EDC/NHS were prepared in 0.10 mol L^{-1} PBS (pH 7.4). The electrode was immersed in this solution for 15 min, under stirring. Then, the immobilization of Anti-PARK7/DJ-1 antibodies (100 μg mL^{-1}) was performed by drop-casting at 4.0 °C (Fig. 1D). 1.0 mg mL^{-1} BSA (Bovine Serum Albumin) was used for the interaction with the NHS residual sites (Fig. 1E). After this step, the antigen-antibody interaction was promoted in the presence of PARK7/DJ-1 protein (antigen) for 1 h (Fig. 1F). The electrode was gently washed and dried with N_2 after each step. Cyclic voltammetry and electrochemical impedance measurements were performed after the immobilization step of known concentrations of the Parkinson's disease-related antigen in 5.0 mmol L^{-1} ferrocene methanol as the redox probe. After use, the immunosensor was stored at 4.0 °C to avoid denaturing the biomolecules, allowing its reuse [28].

3. Results and discussion

3.1. Morphological characterization of 3D-printed electrodes

The morphology of the 3D-printed electrode surfaces was characterized by SEM, AFM, and KPFM. After the activation processes, the electrode surface polymer was removed by the NaOH saponification reaction, uncovering the internal conductive material. According to the literature, the graphene composition in this filament is about 8 13 % [29,30]. As observed by the SEM (Fig. 2A-B) and AFM images (Fig. 2C-D), the electrode surface changed from smooth to rough and irregular morphology. In addition, the presence of nanoribbons structures of about 100 nm in length was also noted, following other previously reported works [14,31]. These structures can be associated with multilayer graphene with the presence of larger interlayer spaces, probably formed throughout the filament thermal extrusion for the 3D printing of the electrodes.

KPFM topography analysis was also performed to understand the changes in the electrode surface after the activation treatments in terms of surface potential (Fig. 2E-F). In this case, the average surface potential calculated for the electrodes decreased from 1.10 to 0.588 V after the proposed pretreatments. This variation suggests the increase of the conductivity of the 3D-printed electrode after the activation treatments, in which the exposure of reduced graphene oxide is reported on the activated 3D-printed electrode [29,32,33]. Also, the specific high-voltage regions can be associated with the low dispersion of charges on the surface, probably due to the presence of oxygenated functional groups on the electrode surface, formed after the electro- chemical activation process. Thus, the morphological results corrobo- rate with the changes observed on the 3D-printed activated electrodes, such as the increase in surface roughness, defects, and conductivity [6, 14].

3.2. Electrochemical behavior of the 3D-printed immunosensor

For the development of the 3D-printed immunosensor, EDC/NHS couple was used for a more stable anti-PARK7/DJ-1 antibodies immobilization on the electrode. EDC/NHS reaction occurs by the EDC interaction with carboxylic groups present on the graphene-based electrode, generated after the electrochemical activation treatments. EDC is substituted by NHS, which presents low stability. The antibody immobilization is done covalently through amine and carboxylic groups bonding on the 3D-printed electrode [34,35]. BSA was used for non-specific site interaction with residual NHS. The antigen-specific interaction occurs, forming the antibody-antigen immunocomplex, which can lead to the blocking of electron transport [13]. All the steps were monitored by CV and EIS measurements, as shown in Fig. 3. After the antibodies immobilization (green line), a peak-to-peak separation (ΔE_p) of 427 35 mV was observed. On the other hand, after the pro- tein incorporation reaction (red line), a slight decrease in the current peaks, as well as an increase of the ΔE_p (604 30 mV), was observed for the cyclic voltammetric response (Fig. 3A). This corroborates with the impedimetric measurements, in which the expected increase of the semi-circle in the Nyquist plot and the charge electron resistance (R_{ct}), from 77.7 ± 5.5 175 ± 10 Ω, were also registered (Fig. 3B). Voltammetric and impedimetric results (i.e., current peak, peak-to-peak separation, and charge electron resistance) obtained after each step for the construction of the 3D printed immunosensor can be compared inFig. S3.

After the antigen-antibody interaction, a more significant difference was noted in both voltammetric and impedimetric responses, indicating the good affinity between antigen and antibody molecules. The results can be correlated to the insulating effect and the blockage of the electron transfer, demonstrating the formation of an insulating layer on the

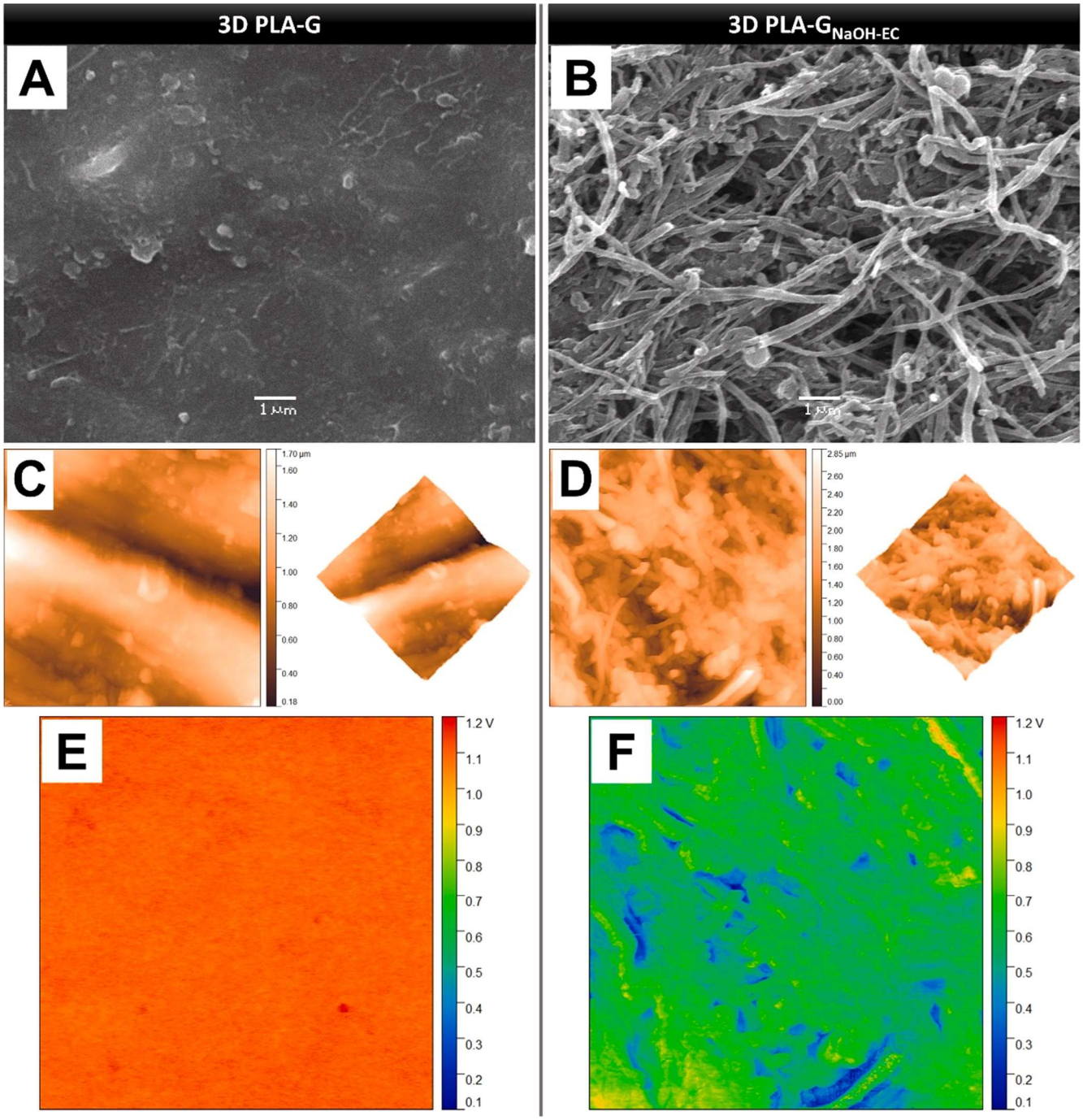

Fig. 2. 3D-printed electrodes morphological characterization: (A, B) SEM, (C, D) AFM, and (E, F) the corresponding KPFM images (10 × 10 µm^2) obtained before (PLA-G) and after activation treatment (PLA-G$_{NaOH-EC}$).

electrode surface [36]. In this case, the antigen-antibody immunocomplex acts as a barrier, compromising the electron transfer and the analytical signal, which agrees with other works reported in the literature [37,38].

3.3. Analytical performance of 3D-printed immunosensor

The analytical performance of the proposed immunosensor was carried out after the interaction of antibodies with antigens at increasing concentration levels. Fig. 4 shows the increase in R_{ct} values proportionally with the increase of PARK7/DJ-1 protein concentrations with a linear region from 5.0 to 200 µg L^{-1} (R^2 = 0.991), corresponding to the equation: ΔR_{ct} (Ω) = 2.53(0.12) $C_{PARK7/DJ-1}$ (µg L^{-1}) + 37.6(3.9). The limits of detection and quantification of 1.01 and 3.38 µg L^{-1} were calculated by the signal-to-noise ratio (LOD: S/N = 3 and LOQ: S/N = 10) [39]. This demonstrates that the proposed immunosensor shows potentiality for the impedimetric detection of DJ-1 protein, related to Parkinson's disease.

Cyclic voltammetric performance of the proposed immunosensor was also carried out for anodic (I_{pa}) and cathodic current peaks (I_{pc}), from 5.0 to 500 µg L^{-1} PARK7/DJ-1 protein (5.0, 50, 100, 200, 300, and 500 µg L^{-1}). Both peaks showed linear behavior for increasing concentrations of protein (Fig. 5), following the equations: ΔI_{pa} (µA) = 0.418 (0.010) $C_{PARK7/DJ-1}$ (µg L^{-1}) + 49.3(0.3) (R^2 = 0.997) and ΔI_{pc} (µA)

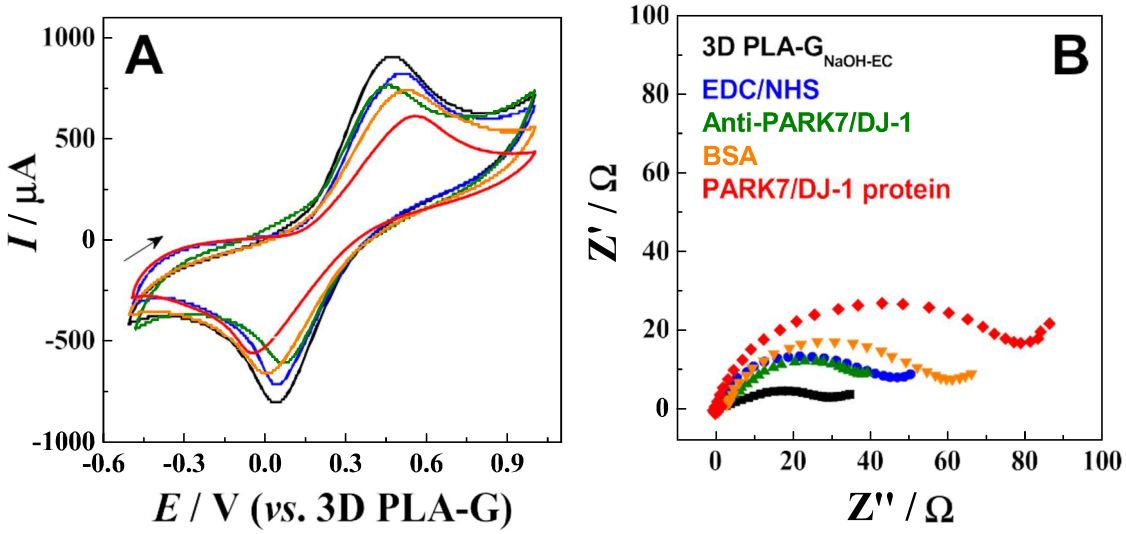

Fig. 3. (A) Cyclic voltammograms and (B) Nyquist plots obtained using the 3D PLA-G_{DMF-EC} electrode before (–●–) and after each step of the biosensor assembly: EDC/NHS activation (–▲–), anti-PARK7/DJ-1 antibodies immobilization (–▼–), BSA immobilization (–♦–), and antibody-protein interaction (–■–). Electrochemical probe: 1.0 mmol L^{-1} FcMeOH.

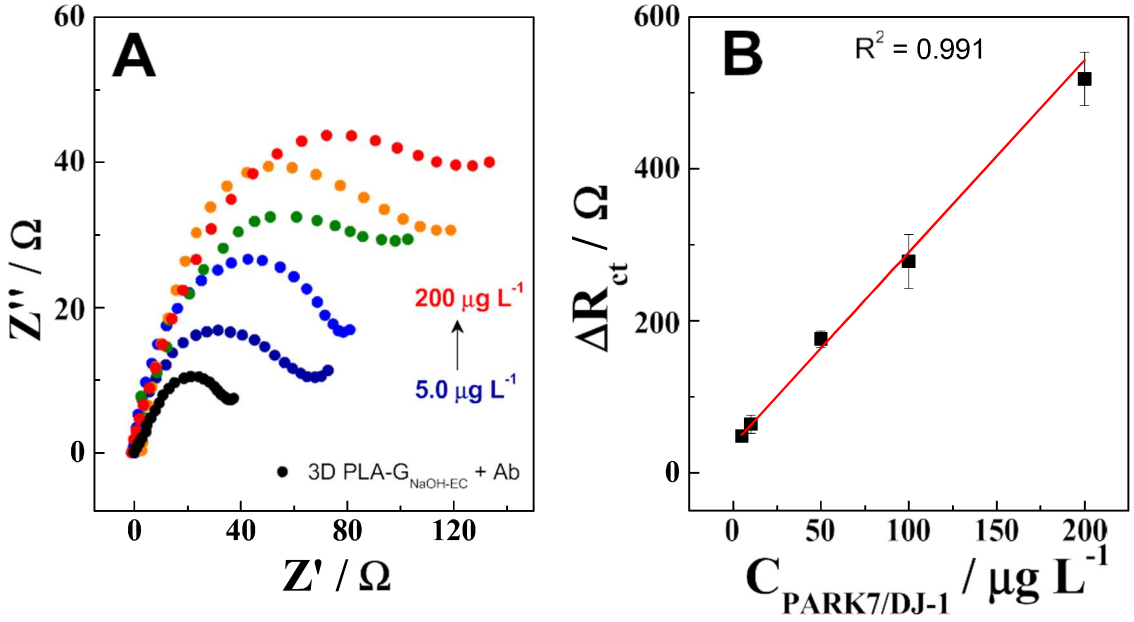

Fig. 4. (A) Nyquist plots and (B) analytical curve obtained for the detection of PARK7/DJ-1 protein at concentrations range of 5.0 – 200 µg L^{-1} for charge transfer resistance (R_{ct}) using the 3D PLA-G_{DMF-EC} electrode. Electrochemical probe: 5.0 mmol L^{-1} FcMeOH. Anti-PARK7/DJ-1 concentration: 100 µg $µL^{-1}$.

= 0.569(0.021) $C_{PARK7/DJ-1}$ (µg L^{-1}) +29.1(6.4) (R^2 =0.993). Limits of detection of 3.46 and 2.69 µg L^{-1} were obtained for the detection of I_{pa} and I_{pc} curves, respectively. Thus, the protein could be detected for any anodic or cathodic peak at different concentration levels, allowing the routine monitoring of the protein and the diagnosis of Parkinson's disease.

The immunosensor showed good repeatability (RSD= 0.803 %) and reproducibility (RSD=5.24 %) for consecutive measurements (n= 6) performed on the same day and different days, respectively (Fig. S4). The proposed 3D-printed pseudo-reference electrode showed good stability during this period with a standard deviation of 15 mV for the anodic peak potential. The stability of the immunosensor was also evaluated by the monitoring of the anodic peak current, in which a decrease of 18.9 % was observed after 25 days using the 3D-printed immunosensor arrangement for the detection of the DJ-1 protein, demonstrating a good stabilization of the electrodes over all the study.

3.4. Detection of PARK7/DJ-1 protein in samples

The proposed sensor was applied for the detection of PARK7/DJ-1 protein in human blood serum and synthetic cerebrospinal fluid samples at three levels of concentration [38,40]. In this sense, the average concentration of DJ-1 protein in patients diagnosticated with Parkinson's disease in different stages (I, II, III, or IV) was found to be approximately 30 ± 8.6 µg L^{-1} [40]. Thus, the proposed immunosensor was successfully applied for the detection of PARK7/DJ-1 protein from altered to normal levels (~ 40 µg L^{-1}). Good recovery values were obtained at three levels of PARK7/DJ-1 protein concentration (30, 40, and 100 µg L^{-1}), as shown in Table 1. This allows even the early diagnosis of Parkinson's disease and/or the routine monitoring of the biomarker for the distinction of the different stages of the disease.

Different configurations of biosensors have been applied for the diagnosis of Parkinson's disease (i.e., GCE, FTO, ITO, SPE, and 3D-

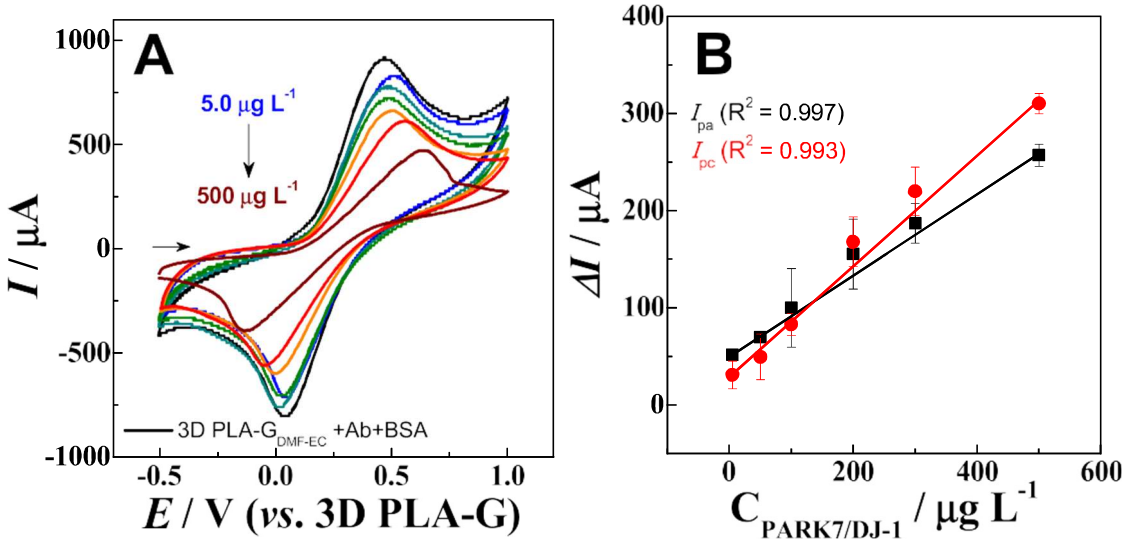

Fig. 5. (A) Cyclic voltammograms and (B) analytical curves obtained for the detection of PARK7/DJ-1 protein at concentrations range of 5.0 500 µg L^{-1} for anodic (I_{pa}, –●–) and cathodic current peaks (I_{pc}, –●–) using the 3D PLA-G_{DMF-EC} electrode. Electrochemical probe: 5.0 mmol L^{-1} FcMeOH. Anti-PARK7/DJ-1 concentration: 100 µg $µL^{-1}$.

Table 1
Determination of PARK7/DJ-1 protein in human blood serum and synthetic cerebrospinal fluid samples (n = 3).

Sample	Added (µg L^{-1})	Found (µg L^{-1})	Recovery (%)
Blood serum	30.0	31.2 ± 3.6	104
	40.0	37.6 ± 3.4	94.0
	100	103 ± 5	103
Cerebrospinal fluid	30.0	30.4 ± 2.4	101
	40.0	41.1 ± 1.2	103
	100	101 ± 3	101

printed sensors) by the detection of targets, such as α-synuclein and DJ-1 protein (Table 2). In this sense, we can highlight that the proposed 3D-printed immunosensor showed great analytical performance for the detection of DJ-1 protein comparable with other biosensors found in the literature, for both voltammetric and impedimetric detections. Furthermore, long-term stability was obtained by using the proposed immunosensor. Finally, we emphasize that the 3D-printing allows the construction of excellent platforms for the stable immobilization of biomolecules, regarding the development of reproductive, reliable, easy construction, and low-cost electrochemical biosensors.

4. Conclusion

We have demonstrated the versatility of 3D printing technology as an interesting platform for the immobilization of biomolecules, aiming for the fabrication of biosensors. An arrangement of 3D-printed electrodes based on PLA and graphene were developed and applied for the detection of PARK7/DJ-1 protein related to Parkinson's disease. A great analytical performance was achieved for the detection of the protein by using both voltammetric and impedimetric techniques with precision and accuracy. The 3D-printed immunosensor arrangement was successfully applied for the detection of the protein in blood serum and cerebrospinal fluid samples allowing even the early diagnosis of Parkinson's disease and/or the routine monitoring of the biomarker in different stages of the disease. This emphasizes that the 3D-printing combined with electrochemical methods allows the development of versatile, reliable, and feasible biosensors.

Table 2
Analytical performance of different immunosensor platforms for the diagnosis of Parkinson's disease.

Sample	Immunosensor	Immobilization	Target	LDR	Slope	LOD	Stability	Ref.
Blood plasma	GCE voltammetric immunosensor	Anti-α-Syn *(EDC/NHS couple)*	α-synuclein	0.05 — 500 pg L^{-1}	2.75 μAL pg^{-1}	0.03 pg L^{-1}	7 days	[41]
Blood serum	FTO voltammetric and impedimetric immunosensor	Anti-α-Syn (cystamine SAM)	α-synuclein	10 — 1000 μg L^{-1}	0.13 μAL μg^{-1} and 2.72 kΩ L μg^{-1}	3.62 and 1.13 μg L^{-1}	7 days	[42]
Blood serum	SPE impedimetric immunosensor	Anti-DJ-1 (cysteamine-glutaraldehyde binding)	DJ-1 protein	40 — 150 μg L^{-1}	4.85 Ω L μg^{-1}	7.5 μg L^{-1}	—	[38]
Cerebrospinal fluid and saliva	ITO voltammetric and impedimetric immunosensor	Anti-DJ-1 (SAM)	DJ-1 protein	4.7–4700 pg L^{-1}	–	0.50 pg L^{-1}	5 weeks	[43]
N2A cells	MIP/SPCE voltammetric and impedimetric immunosensor	Anti-DJ-1 (SAM)	DJ-1 protein	1.0 – 500 nmol L^{-1}	0.025 μAL $nmol^{-1}$ and 0.17 kΩ L $nmol^{-1}$	1.0 nmol L^{-1}	—	[44]
Blood serum and cerebrospinal fluid	*3D-printed voltammetric and impedimetric immunosensor*	*Anti-DJ-1 (EDC/NHS couple)*	*DJ-1 protein*	*5.0–500 μg L^{-1}*	*0.57 μAL μg^{-1} and 2.53 ΩL μg^{-1}*	*2.69 and 1.01 μg L^{-1}*	*25 days*	*This work*

Writing e original draft, Writing – review & editing, **Craig E. Banks:** Conceptualization, Methodology, Resources, Supervision, Visualization, Writing – review & editing., **Bruno Campos Janegitz:** Conceptualiza- tion, Funding acquisition, Project administration, Methodology, Re- sources, Supervision, Visualization, Writing – review & editing, **Juliano Alves Bonacin:** Conceptualization, Funding acquisition, Project administration, Methodology, Resources, Supervision, Visualization, Writing – review & editing.

Declaration of Competing Interest

The authors declare that they have no known competing financial interests or personal relationships that could have appeared to influence the work reported in this paper.

Data Availability

Data will be made available on request.

Acknowledgments

This study was financed in part by the Coordenação de Aperfeiçoamento de Pessoal de Nível Superior, CAPES (Finance Code 001, Pandemias 88887.504861/2020-00 and 88887.712315/2022-00), São Paulo Research Foundation, FAPESP (grants #2021/07989-4, 2019/00473-2, 2019/01844-4, 2017/21097-3, and 2013/22127-2, Conselho Nacional de Desenvolvimento Científico e Tecnológico, CNPq (303338/2019-9 and 308203/2021-6).

Appendix A. Supporting information

Supplementary data associated with this article can be found in the online version

References

[1] A. Kalkal, S. Kumar, P. Kumar, R. Pradhan, M. Willander, G. Packirisamy, S. Kumar, B.D. Malhotra, Recent advances in 3D printing technologies for wearable (bio) sensors, Addit. Manuf. 46 (2021), 102088.
[2] R.M. Cardoso, C. Kalinke, R.G. Rocha, P.L. Santos, D.P. Rocha, P.R. Oliveira, B. C. Janegitz, J.A. Bonacin, E.M. Richter, R.A.A. Munoz, Additive-manufactured (3D-printed) electrochemical sensors: a critical review, Anal. Chim. Acta, 1118 (2020) 73–91.
[3] J. Muñoz, M. Pumera, 3D-printed biosensors for electrochemical and optical applications, TrAC Trends Anal. Chem. 128 (2020), 115933.
[4] R.S. Shergill, A. Farlow, F. Perez, B. Patel, 3D-printed electrochemical pestle and mortar for identification of falsified pharmaceutical tablets, Microchim. Acta 189 (3) (2022) 1–10.
[5] Bhaiyya, M.; Pattnaik, P.K.; Goel, S. Smartphone Integrated 3D-Printed Standalone Electrochemiluminescence Platform for Cholesterol Detection. in *2022 IEEE International Symposium on Medical Measurements and Applications (MeMeA)*: 2022.
[6] Crapnell, R.D.; Bernalte, E.; Ferrari, A.G.-M.; Whittingham, M.J. Williams, R.J.; Hurst, N.J. Banks, C.E. All-in-One Single-Print Additively Manufactured Electroanalytical Sensing Platforms. *ACS Measurement Science Au*, 2021.
[7] V. Katseli, M. Angelopoulou, C. Kokkinos, 3D printed bioelectronic microwells, Adv. Funct. Mater. 31 (26) (2021) 2102459.
[8] E.M. Richter, D.P. Rocha, R.M. Cardoso, E.M. Keefe, C.W. Foster, R.A. Munoz, C. E. Banks, Complete additively manufactured (3D-printed) electrochemical sensing platform, Anal. Chem. 91 (20) (2019) 12844–12851.
[9] J.S. Stefano, C. Kalinke, R.G. Da Rocha, D.P. Rocha, V.A.O.P. Da Silva, J. A. Bonacin, L.C. Angnes, E.M. Richter, B.C. Janegitz, R.A.A. Munoz, Electrochemical (Bio) sensors enabled by fused deposition modeling-based 3D printing: a guide to selecting designs, printing parameters, and post-treatment protocols, Anal. Chem. (2022).
[10] X. Wang, M. Jiang, Z. Zhou, J. Gou, D. Hui, 3D printing of polymer matrix composites: a review and prospective, Compos. Part B: Eng. 110 (2017) 442–458.
[11] A. Akbari, M. Jawaid, A. Hassan, H. Balakrishnan, Epoxidized natural rubber toughened polylactic acid/talc composites: mechanical, thermal, and morphological properties, J. Compos. Mater. 48 (7) (2013) 769–781.
[12] C. Kalinke, P.R. De Oliveira, N.V. Neumsteir, B.F. Henriques, G. De Oliveira Aparecido, H.C. Loureiro, B.C. Janegitz, J.A. Bonacin, Influence of filament aging and conductive additive in 3D printed sensors, Anal. Chim. Acta 1191 (2022), 339228.
[13] G. Martins, J.L. Gogola, L.H. Budni, B.C. Janegitz, L.H. Marcolino-Junior, M. F. Bergamini, 3D-printed electrode as a new platform for electrochemical immunosensors for virus detection, Anal. Chim. Acta 1147 (2021) 30–37.
[14] C. Kalinke, N.V. Neumsteir, G.O. Aparecido, T.V.B. Ferraz, P.L. Santos, B. C. Janegitz, J.A. Bonacin, Comparison of activation processes for 3D printed PLA-graphene electrodes: electrochemical properties and application for sensing of dopamine, Analyst 145 (4) (2020) 1207–1218.
[15] D.P. Rocha, R.G. Rocha, S.V. Castro, M.A. Trindade, R.A. Munoz, E.M. Richter, L. Angnes, Posttreatment of 3D-printed surfaces for electrochemical applications: a critical review on proposed protocols, Electrochem. Sci. Adv. (2021), e2100136.
[16] R.M. Cardoso, P.R.L. Silva, A.P. Lima, D.P. Rocha, T.C. Oliveira, T.M. Do Prado, E. L. Fava, O. Fatibello-Filho, E.M. Richter, R.A.A. Muñoz, 3D-Printed graphene/polylactic acid electrode for bioanalysis: biosensing of glucose and simultaneous determination of uric acid and nitrite in biological fluids, Sens. Actuators B: Chem. 307 (2020), 127621.
[17] A. Roda, M. Guardigli, D. Calabria, M.M. Calabretta, L. Cevenini, E. Michelini, A 3D-printed device for a smartphone-based chemiluminescence biosensor for lactate in oral fluid and sweat, Analyst 139 (24) (2014) 6494–6501.
[18] R.D. Crapnell, W. Jesadabundit, A. Garcia-Miranda Ferrari, N.C. Dempsey-Hibbert, M. Peeters, A. Tridente, O. Chailapakul, C.E. Banks, Toward the rapid diagnosis of sepsis: detecting Interleukin-6 in blood plasma using functionalized screen-printed electrodes with a thermal detection methodology, in: Analytical Chemistry, 93, 2021, pp. 5931–5938.
[19] R. Suvanasuthi, S. Chimnaronk, C. Promptmas, 3D printed hydrophobic barriers in a paper-based biosensor for point-of-care detection of dengue virus serotypes, Talanta 237 (2022), 122962.
[20] J.S. Stefano, L.R. Guterres e Silva, R.G. Rocha, L.C. Brazaca, E.M. Richter, R. A. Abarza Muñoz, B.C. Janegitz, New conductive filament ready-to-use for 3D-printing electrochemical (bio)sensors: towards the detection of SARS-CoV-2, Anal. Chim. Acta 1191 (2022), 339372.
[21] S. Damiati, S. Küpcü, M. Peacock, C. Eilenberger, M. Zamzami, I. Qadri, H. Choudhry, U.B. Sleytr, B. Schuster, Acoustic and hybrid 3D-printed electrochemical biosensors for the real-time immunodetection of liver cancer cells (HepG2), Biosens. Bioelectron. 94 (2017) 500–506.
[22] L. He, S. Lin, H. Pan, R. Shen, M. Wang, Z. Liu, S. Sun, Y. Tan, Y. Wang, S. Chen, J. Ding, Lack of Association Between DJ-1 Gene Promoter Polymorphism and the Risk of Parkinson's Disease 11 (2019) 24.
[23] T. Kinumi, J. Kimata, T. Taira, H. Ariga, E. Niki, Cysteine-106 of DJ-1 is the most sensitive cysteine residue to hydrogen peroxide-mediated oxidation in vivo in human umbilical vein endothelial cells, Biochem. Biophys. Res. Commun. 317 (3) (2004) 722–728.
[24] Y. Saito, DJ-1 as a biomarker of Parkinson's disease. DJ-1/PARK7 Protein, ed, Springer, 2017, pp. 149–171.
's disease,
K.-H. Chang, C.-M. Chen, The role of oxidative stress in Parkinson
Antioxidants 9 (7) (2020) 597.
[26] R. De Toledo, M.C.D. Santos, E. Cavalheiro, L. Mazo, Determination of dopamine in synthetic cerebrospinal fluid by SWV with a graphite – polyurethane composite electrode, Anal. Bioanal. Chem. 381 (6) (2005) 1161–1166.
[27] C. Kalinke, N.V. Neumsteir, P.R. Oliveira, B.C. Janegitz, J.A. Bonacin, Sensing of L-methionine in biological samples through fully 3D-printed electrodes, Anal. Chim. Acta 1142 (2021) 135–142.
[28] M.H. Nawaz, A. Hayat, G. Catanante, U. Latif, J.L. Marty, Development of a portable and disposable NS1 based electrochemical immunosensor for early diagnosis of dengue virus, Anal. Chim. Acta 1026 (2018) 1–7.
[29] P.L. Dos Santos, V. Katic, H.C. Loureiro, M.F. Dos Santos, D.P. Dos Santos, A.L. B. Formiga, J.A. Bonacin, Enhanced performance of 3D printed graphene electrodes after electrochemical pre-treatment: role of exposed graphene sheets, Sens. Actuators B: Chem. 281 (2019) 837–848.
[30] C.W. Foster, H.M. Elbardisy, M.P. Down, E.M. Keefe, G.C. Smith, C.E. Banks, Additively manufactured graphitic electrochemical sensing platforms, Chem. Eng. J. 381 (2020), 122343.
[31] R.M. Cardoso, S.V. Castro, M.N. Silva, A.P. Lima, M.H. Santana, E. Nossol, R. A. Silva, E.M. Richter, T.R. Paixão, R.A. Munoz, 3D-printed flexible device combining sampling and detection of explosives, Sens. Actuators B: Chem. 292 (2019) 308–313.
[32] M. Santhiago, C.M. Maroneze, C.C. Silva, M.N. Camargo, L.T. Kubota, Electrochemical oxidation of glassy carbon provides similar electrochemical response as graphene oxide prepared by tour or hummers routes, ChemElectroChem 2 (5) (2015) 761–767.
[33] V. Katic, P.L. Santos, M.F. Santos, B.M. Pires, H.C. Loureiro, A.P. Lima, J. C. Queiroz, R. Landers, R.A. Munoz, J.A. Bonacin, 3D printed graphene electrodes modified with prussian blue: emerging electrochemical sensing platform for peroxide detection, ACS Appl. Mater. Interfaces 11 (38) (2019) 35068–35078.
[34] R.A. Blaik, E. Lan, Y. Huang, B. Dunn, Gold-Coated M13 bacteriophage as a template for glucose oxidase biofuel cells with direct electron transfer, ACS nano 10 (1) (2016) 324–332.
[35] D. Yun, M. Song, S. Hong, M. Kang, N. Min, Highly sensitive and renewable amperometric urea sensor based on self-assembled monolayer using porous silicon substrate, J.-KOREAN Phys. Soc. 47 (2005) S445.
[36] B. Mojsoska, S. Larsen, D.A. Olsen, J.S. Madsen, I. Brandslund, F.A. Alatraktchi, Rapid SARS-CoV-2 detection using electrochemical immunosensor, Sensors 21 (2) (2021) 390.
[37] G. Martins, J.L. Gogola, F.R. Caetano, C. Kalinke, T.R. Jorge, C.N. Santos, M. F. Bergamini, L.H. Marcolino-Junior, Quick electrochemical immunoassay for hantavirus detection based on biochar platform, Talanta 204 (2019) 163–171.

[25]

[38] G.C.M.D. Oliveira, J.H.D.S. Carvalho, L.C. Brazaca, N.C.S. Vieira, B.C. Janegitz, Flexible platinum electrodes as electrochemical sensor and immunosensor for Parkinson's disease biomarkers, Biosens. Bioelectron. 152 (2020), 112016.
[39] J. Miller, J.C. Miller, Statistics and Chemometrics for Analytical Chemistry, Pearson education, 2018.
[40] Z. Hong, M. Shi, K.A. Chung, J.F. Quinn, E.R. Peskind, D. Galasko, J. Jankovic, C. P. Zabetian, J.B. Leverenz, G.J.B. Baird, DJ-1 and α -synuclein in human cerebrospinal fluid as biomarkers of Parkinson's disease 133 (3) (2010) 713–726.
[41] D. Tao, Y. Gu, S. Song, E.P. Nguyen, J. Cheng, Q. Yuan, H. Pan, N. Jaffrezic-Renault, Z. Guo, Ultrasensitive detection of alpha-synuclein oligomer using a PolyD-glucosamine/gold nanoparticle/carbon-based nanomaterials modified electrochemical immunosensor in human plasma, Microchem. J. 158 (2020), 105195.
[42] C.-Y. Ge, M.M. Rahman, W. Zhang, N.S. Lopa, L. Jin, S. Yoon, H. Jang, G.-R. Xu, W. Kim, An electrochemical immunosensor based on a self-assembled monolayer modified electrode for label-free detection of α -synuclein, Sensors 20 (3) (2020) 617.
[43] M.N. Sonuç Karaboğa, M.K. Sezgintürk, A nano-composite based regenerative neuro biosensor sensitive to Parkinsonism-associated protein DJ-1/Park7 in cerebrospinal fluid and saliva, Bioelectrochemistry 138 (2021), 107734.
[44] Kumar, M.D.; Karunakaran, C.; Karthikeyan, M.; Sharma, N. Kalivendi, S.V. Raju, V.; Vatsalarani, J. Molecular Imprinting Synthetic Receptor Based Sensor for Determination of Parkinson's Disease Biomarker DJ-1. *SSRN*, 2022.